Supplementary Materials for

Direct stimulation of $NADP^+$ synthesis through Akt-mediated phosphorylation of NAD kinase

Gerta Hoxhaj, Issam Ben-Sahra, Sophie E. Lockwood, Rebecca C. Timson, Vanessa Byles, Graham T. Henning, Peng Gao, Laura M. Selfors, John M. Asara, Brendan D. Manning*

*Corresponding author. Email: bmanning@hsph.harvard.edu

Published 8 March 2019, *Science* **363**, 1088 (2019)
DOI: 10.1126/science.aau3903

This PDF file includes:

Materials and Methods
Figs. S1 to S8
Tables S1 and S2
References

Materials and Methods:

Antibodies and other reagents

Antibodies to phospho (p)-Akt-S473 (Cell Signaling Technology (CST), 4060), Akt (CST, 4691), NADK (CST, 55948), p-RRXpS/pT (CST, 9624), p-S6K1-T389 (CST, 9234), p-S6-S240/S244 (CST, 2215), p-TSC2-T1462 (CST, 3617), p-PRAS40-T246 (CST, 2997), horse radish peroxidase (HRP)-conjugated secondary antibodies anti-mouse (CST, 7076) and anti-rabbit (CST, 7074), anti-FLAG M2 Affinity Gel (Sigma, A2220), anti-FLAG-M2 (Sigma, F1804), anti-HA (Sigma, H3663), β-actin (Sigma, A5316), thiazolyl Blue Tetrazolium Bromide solution (Sigma, M5655), anti-G6PD (Bethyl A300-404A), anti-C5ORF33(NADK2) (Abcam, ab181028) and IRDye 800CW Donkey anti-Mouse IgG (H+L) (Licor, 926-32212) were used. Anti-sera for p-NADK-Ser44/46 (antibodies under development) were provided by CST. Note: the NADK antibody validated by siRNA knockdown (CST, 55948) does not recognize NADK derivatives lacking the N-terminal domain. Thus, immunoblots for experiments using the ΔN-NADK or isoform 3 variants used a different validated NADK antibody (Sigma HPA048909), raised against sequences within the kinase domain.

Human Insulin-like Growth Factor I (IGF-I), (CST #8917), insulin (Alpha diagnostic, INSL16-N-5), LPS (Invivogen, tlrl-eklps), Akt inhibitor MK-2206 (Selleckchem, S1078), mTORC1 inhibitor rapamycin (LC laboratories, R-5000), mTOR inhibitor Torin1 (Tocris, 4247), PI3K inhibitor GDC-0941 (Selleckchem, S1065), PDK1 inhibitor GSK2334470 (SelleckChem, S7087), ATP-competitive Akt inhibitor GSK690693 Selleckchem, S1113), NAMPT inhibitor FK 866 hydrochloride (Tocris, 480810), β-nicotinamide adenine dinucleotide hydrate (NAD) (Sigma, N7004), D-glucose 6-phosphate disodium salt hydrate (G6P) (Sigma, G7250), glucose-

6-phosphate dehydrogenase from baker's yeast (G6PD) (Sigma, G6378), adenosine triphosphate salt (ATP) (Sigma, A2383), NADP/NADPH kit (Sigma, MAK038), β-nicotinamide adenine dinucleotide phosphate hydrate (NADP) (Sigma, N5755), β-nicotinamide adenine dinucleotide phosphate, reduced tetra (cyclohexylammonium) salt (NADPH) (Sigma, N5130), folic acid (Sigma, F7876), pyridoxal hydrochloride (Sigma, P6155), riboflavin (Sigma, R9504), protease inhibitor cocktail (Sigma, P8340), IPTG (Sigma, I6758), DTAB (Sigma, D8638), Trizma® base (Sigma, T1503), Benzonase ® nuclease (Sigma, E1014), NADP/NADPH-Glo™ Assay (Promega, G9081), $^{13}C_{3}{}^{15}N$-nicotinamide (Cambridge Isotope Labs, CNLM-9757-0.001), [γ-32P]-ATP (Perkin Elmer, BLU002A100UC), Lipofectamine RNAiMAX (ThermoFisher Scientific, 13778), Lipofectamine 3000 Transfection Reagent (Thermo Fischer, L3000015), lysozyme (Thermo, 89833), HEPES (Thermo, 15630080), Glutathione (Thermo, 78259), sodium pyruvate (Thermo, 11360-070), Corning® glutagro™ (Corning, 25-015-CI), Gibco™ 2-mercaptoethanol (Gibco, 21985023), BCA kit (Thermo, 23225), hygromycin B (Life Technologies/Invitrogen, 10687-010), polyethylenimine (PEI) (Polysciences, 23966-2), nicotinamide-free DMEM (US biologicals, D9800-17), thiamine hydrochloride (Santa Cruz, sc-205859), polybrene (Santa Cruz, sc-134220), KOD Xtreme™ Hot Start DNA Polymerase (Millipore, 71975-3), Lonza SeaPlaque® Agarose (VWR, 50101), Microcystin-LR (Enzo life sciences, ALX-350-012-C500), Bradford assay reagent (Bio-Rad) and dialyzed serum (dFBS; Life Technologies/Gibco, 26400-036) were used as indicated. Recombinant active PKB alpha (AKT1)-S473D (aa 118 - 480) (DU1850) and SGK inhibitor 14h were from MRC Protein Phosphorylation Unit Reagents and Services, University of Dundee.

Cell culture

HEK293E (gift of Carol Mackintosh), immortalized ($p53^{-/-}$) MEF (gift of David Kwiatkowski), and U87MG (ATCC) cell lines were maintained in Dulbecco's Modified Eagle's Medium (DMEM; Corning/Cellgro, 10-017-CV) containing 10% fetal bovine serum (FBS). MDA-MB-468 (ATCC), LnCAP (ATCC), T47D (ATCC), and A549 (ATCC) were maintained in RPMI-1640 (Corning, 10-040-CV) with 10% FBS. MCF10A cells expressing Akt2 or oncogenic Akt2-E17K in a doxycycline-inducible manner (gift of Alex Toker) were cultured as described previously (*12*). For insulin or IGF1 stimulation, subconfluent cells were serum-starved in DMEM for 16 hours and then stimulated with 0.5 μM insulin or 100 ng/ml IGF1 for the indicated times. Where indicated, cells were incubated with inhibitors 30 min prior to insulin or IGF1 stimulations. Bone marrow-derived macrophages (BMDMs) were prepared as described previously (*13*). 1.5 x 10^6 BMDMs were plated in each well of a 6-well plate in RPMI media supplemented with 10% FBS, 1X Pen/Strep, 1X Corning® glutagro™, 1X HEPES, 1X sodium pyruvate and 1X beta mercaptoethanol. 16 h post-plating, cells were pretreated with inhibitors and stimulated with LPS, as indicated.

cDNA constructs, RNAi, and CRISPR/Cas9

HA-AKT-CA (myristoylated-Akt) and HA-AKT-KD (Akt^{K179D}) were expressed from $pcDNA3.1^+$. Full-length human NADK isoform 1 (RC200544) and NADK isoform 3 (RC231219) cDNAs in the pCMV6-entry vector were purchased from Origene. NADK variants S44A, S46A, S48A, S44/S46A, S44/S46/S48A, ΔN (aa 1-87) NADK were generated by Dpn I-mediated site-directed mutagenesis using KOD Xtreme™ Hot Start DNA Polymerase, with mutations verified by sequencing. NADK and its variants were FLAG-tagged at the C-terminus

during PCR-based subcloning into the pGEX-6P-1 vector for bacterial expression as a GST fusion and in the pBabe-Hygro retroviral vector (HEK293E) or pSMPUW-IRES-Hygro lentiviral vector (Cell biolabs, VPK-217; U87MG) for generation of stable human cell lines. All final constructs were sequence verified. For transient expression, NADK variants in the pCMV6 vector were used, with PEI transfection of 4 μg of plasmid DNA, and experiments were initiated 24 h post-transfection.

SmartVector Non-targeting shRNA (VSC11651) and an Inducible mCMV-TurboRFP human NADK shRNA targeting the NADK 3'UTR (V3SH11252-225668231; Dharmacon) were used to generate stable cell lines (HEK293E and U87MG) expressing control shRNAs or those targeting NADK in a doxycyline (dox)-inducible manner via lentivirus delivery and puromycin (2 μg/ml) selection. The resulting stable dox-inducible NADK knockdown cell lines were used to generate stable NADK-reconstituted cell lines using the retroviral or lentiviral NADK expression vectors described above following hygromycin (200 μg/ml) selection. shRNAs were induced with dox (0.25 μg/ml) 24 h before plating for experiments and then continued for the duration of the experiment, unless otherwise indicated.

T47D and A549 cells expressing control shRNA (pLKO.1-puro) or shRNA targeting NADK (Sigma: TRCN0000199040) were generated via lentivirus delivery and puromycin (3 μg/ml) selection. These resulting stable cell lines were used to generate stable NADK-reconstituted cell lines using lentiviral NADK expression vectors (pSMPUW-IRES-Hygro) following hygromycin (300 μg/ml) selection.

For transient siRNA-mediated knockdowns involving metabolite extraction and analyses, 20 nM ON-TARGETplus siRNA pools (Dharmacon) were transfected into cultures on 10-cm dishes with 30 µl Lipofectamine RNAiMAX for 48 h, according to the manufacturers' instructions.

To generate HEK293E NADK knockout cells, an sgRNA sequence targeting the second exon of NADK was cloned into the PX459 CRISPR (Addgene, Plasmid #48139) vector using the following guides: Sense: AACTCCAGGTCTCATCGCCG, Antisense: CGGCGATGAGACCTGGAGTT. Two days post-transfection, cells were subjected to puromycin selection (2 µg/ml, 48 hours) and seeded into 96-well plates as single cells using a limiting dilution method. Clonal cells were screened by immunoblotting with an NADK antibody.

Immunoblotting and immunoprecipitation.

For protein extracts, cells were lysed in ice-cold 1% Triton lysis buffer (40 mM HEPES, pH 7.4, 120 mM NaCl, 1 mM EDTA, 1% Triton X-100, 10 mM sodium pyrophosphate, 10 mM glycerol 2-phosphate, 50 mM NaF, 0.5 mM sodium orthovanadate) with 1 µM Microcystin-LR and protease inhibitor cocktail added just prior to cell lysis. Lysates were clarified by centrifugation (20,000 x *g* for 15 min at 4^{o}C) and protein concentrations were determined with Bradford assay. Normalized protein lysates were subjected to SDS-PAGE followed by transferring to nitrocellulose membranes and immunoblotting with the indicated antibodies. For detection of endogenous NADK phosphorylation via immunoblot with the phospho-NADK-S44/46 antibody, 50µg of protein lysates were loaded on 4–15% Criterion™ TGX™ Precast gradient gels. Most

proteins were detected using enhanced chemiluminescence (ECL), while β-actin loading controls were detected using the Odyssey® CLx-Imaging System (LI-COR Biosciences).

For immunoprecipitation of FLAG-tagged NADK, cell lysates (2 mg) were incubated with 30 µl of a 50% slurry of anti-FLAG M2 Affinity Gel for 3 hours. Beads were washed with lysis buffer four times and washed once with equilibration buffer (10 mM HEPES, 50 mM NaCl, protease inhibitors and 1 µM Microcystin-LR). After completely removing the equilibration buffer, the NADK-FLAG was eluted in 40 µl elution buffer (0.2 mg/ml 3xFLAG peptide, 10 mM HEPES, 50 mM NaCl, protease inhibitors and 1 µM Microcystin-LR) for 1 hour at 4^{o}C. The eluate was passed through 0.45 µm Costar® Spin-X® Centrifuge Tube Filters. 10 µl of 6X Laemmli sample buffer was added to the eluates. These samples were then used for immunoblotting with phospho-motif or phospho-NADK-S44/S46.

Measurements of NADP^{+} and NADPH using a colorimetric enzyme-based assay

NADP^{+} and NADPH were measured using a modified NADP/NADPH colorimetric quantification assay (Sigma, MAK038), which involves an NADP^{+}-cycling enzyme that converts all NADP^{+} to NADPH for spectrophotometric detection at A450 nm. An important modification to the manufacturer's protocol was used, as we found that measurements made directly on samples prepared with the provided extraction buffer gave highly variable results. Instead, we quantified NADP/NADPH concentrations in metabolite extracts, prepared as described previously (*14*). Briefly, metabolite extraction from a 10 cm culture dish per sample was performed on dry ice with 80% methanol, and supernatants were dried down under nitrogen gas. Metabolites were then resuspended in 200 µl of the manufacturer's extraction buffer and

centrifuged for 2 min at 3000g. Each sample supernatant was split in half. One half (A) was subjected to incubation at 60°C for 30 minutes to decompose $NADP^+$, leaving only NADPH. The other half (B), containing NADP and NADPH, was left on ice for 30 min. Split samples A and B were transferred to clear-bottom 96-well plates and the $NADP^+$-cycling enzyme was added to each for 5 min, resulting in conversion of NADP in sample B to NADPH, followed by addition of the manufacture's NADPH developing solution. NADPH was continuously monitored at 450 nm every 15 min for 2 hours. For each assay, an NADPH standard with 0, 20, 40, 60, 80, and 100 pmole/well was included. The amount of NADPH in an unknown sample was calculated from the standard curve. $NADP^+$ concentrations are equal to the difference between sample B and A. For normalization of each sample, the insoluble pellet from the metabolite extractions were solubilized with 8 M urea in 10 mM Tris (pH 8) and protein was quantified with a BCA assay kit. The data is presented as relative abundance and each data point is the average of at least four biological replicates of at least two independent experiments. A validation experiment for this assay demonstrating accurate quantification of $NADP^+$ and NADPH in both pure samples and a 1:1 mixture is provided in Fig. S1A. Figures 1A, B, C and figure S1A, B show data using this method.

Measurements of $NADP^+$ and NADPH using a bioluminescent enzyme-based assay

$NADP^+$ and NADPH were also measured using NADP/NADPH-Glo™ Assay (Promega) according to the manufacturer's protocol. $NADP^+$ and NADPH are measured separately, based on their differential stabilities in acidic and basic pH (i.e. NADP is unstable in basic solution while NADPH is unstable in acidic solution). Briefly, cells grown in 6-well plates were washed twice with PBS and then resuspended in 500 µl of PBS. Cells were lysed by mixing 100 µl of the

PBS-resuspended cells with 100 µl of base solution (0.2N NaOH with 1% DTAB). For $NADP^+$ measurement (acid treatment), 25 µl of 0.4N HCl was added to 50 µl of the lysed samples, which were then incubated for 15 minutes at 60°C. Simultaneously, 50 µl of the original lysed sample (base-treated) were also incubated for 15 minutes at 60°C. After heat-treatment the samples were equilibrated at room temperature for 10 minutes before neutralizing the acid-treated cells with 25 µl of 0.5M Trizma® base solution and the base-treated cells with 50 µl of HCl/Trizma solution (1:1 volume of 0.4N HCl and 0.5M Trizma® base).100 µl of each acid- and basic-treated samples were added to 96-well white luminometer plates and the reaction was started by addition of 100 µl of NADP/NADPH-Glo™ Detection Reagent. The reaction was incubated for 1 hour before the luminescence was recorded. Standard curves were generated using purified $NADP^+$ and NADPH prepared in the same buffers used to prepare the experimental samples. The amount of $NADP^+$ and NADPH of each samples were calculated using the standard curve. For normalization of each sample, 100 µl of the PBS resuspended cells were pelleted and resuspended in 8 M urea in 10 mM Tris (pH 8) and protein was quantified with a BCA assay kit. The data is presented as relative abundance and each data point is the average of five biological replicates. A validation experiment for this assay is shown in Fig. S1C. The data shown in figure S1D use this method.

LC-MS/MS-based metabolite profiling and $^{13}C_3{}^{15}N$-nicotinamide tracing

To determine the relative abundance of pyridine metabolites by LC-MS/MS analyses, a previously described extraction method optimized for NADP and NADPH was employed (*15*). Briefly, cells cultured in 10 cm plates to ~90% confluence were washed twice with cold PBS and metabolites were extracted on ice with 800 µl of a 40:40:20 mixture of Acetonitrile/Methanol/

(10 mM Tris, pH 9.2, 200 mM NaCl). Cells were scraped and placed at -80°C for 1 hour before centrifugation at 17000g for 5 min. Supernatants were stored at -80°C (one week or less) and 25 µl of the cleared solution was injected in a Thermo Q-Exactive (LC-MS) in line with an electrospray source and an Ultimate3000 (Thermo) series HPLC consisting of a binary pump, degasser, and auto-sampler outfitted with a Xbridge Amide column (Waters; dimensions of 4.6 mm × 100 mm and a 3.5 µm particle size). The mobile phase A contained 95% (vol/vol) water, 5% (vol/vol) acetonitrile, 20 mM ammonium hydroxide, 20 mM ammonium acetate, pH 9.0; B was 100% Acetonitrile. The gradient was as follows: 0 min, 15% A; 2.5 min, 30% A; 7 min, 43% A; 16 min, 62% A; 16-18 min, 75% A; 18-25 min, 15% A with a flow rate of 400 µl/min. The capillary of the ESI source was set to 275°C, with sheath gas at 45 arbitrary units, auxiliary gas at 5 arbitrary units and the spray voltage at 4.0 kV. In positive/negative polarity switching mode, an m/z scan range from 70 to 850 was chosen and MS1 data was collected at a resolution of 70,000. The automatic gain control (AGC) target was set at 1×10^6 and the maximum injection time was 200 ms. The top 5 precursor ions were subsequently fragmented, in a data-dependent manner, using the higher energy collisional dissociation (HCD) cell set to 30% normalized collision energy in MS2 at a resolution power of 17,500. Data acquisition and analysis were carried out by Xcalibur 4.0 software and Tracefinder 2.1 software, respectively (both from Thermo Fisher Scientific). Selective ion monitoring (SIM) of metabolites measured in stable isotopic tracing experiments are listed in Table S1. Alternatively, for steady state analysis of metabolites (fig. S2A), dried pellets were re-suspended in 20 µL HPLC-grade water for mass spectrometry and 10 µl of the samples were injected into a 5500 QTRAP hybrid triple quadrupole mass spectrometer (AB/SCIEX) coupled to a Prominence UFLC HPLC system (Shimadzu) with Amide XBridge HILIC chromatography (Waters) via selected reaction

monitoring (SRM) and polarity switching between positive and negative modes (*16*). For all extractions, the remaining pellets were resuspended in 8 M Urea /10 mM Tris, pH 8, heated at 60°C degrees for 1 hour with shaking, centrifuged, and protein concentration in the supernatant was quantified using BCA kit. For [$^{13}C_3{}^{15}N$]-nicotinamide tracing studies, cells were washed once with serum- and nicotinamide-free DMEM and then incubated in the same medium containing 4 mg/L of $^{13}C_3{}^{15}N$-nicotinamide for 1 hour or 30 min, as indicated. In experiments in which inhibitors and growth factors were used, cells were pretreated for 30 min with inhibitors prior to co-addition of growth factors in nicotinamide-free DMEM containing $^{13}C_3{}^{15}N$-nicotinamide. The nicotinamide-free media containing labeled nicotinamide was prepared using powdered DMEM (USBiological Life Sciences, D9815) supplemented with standard DMEM concentrations of Folic Acid, Niacinamide, Pyridoxal, Riboflavin, Thiamine, Glucose, Sodium Pyruvate, and, in the place of nicotinamide, $^{13}C_3{}^{15}N$-nicotinamide, pH adjusted to 7.2.

mRNA expression analysis

For mRNA expression quantification, total cellular RNA was isolated with an RNeasy kit (Qiagen) from cells grown to near confluency grown in 6-well plates. cDNA was generated from 1 µg of total RNA using the RNA to cDNA EcoDry™ Premix (Takara, 639545), diluted in nuclease free water (1:10) before quantification by real-time PCR using a Biorad CFX Connect Real-Time PCR Detection System. Each reaction contains 5 ng of cDNA, SYBR Green PCR mix (SYBR Green Master Mix®, Biorad) and the specified primers (Table S3). Transcript levels for NADK and NADK2 were normalized to control RPLP0 transcript levels and the data was presented as fold change relative to the average of the control samples. Each sample presented is

the average of three biological triplicates measured in technical triplicates. The data is representative of two independent experiments. The primer sequences are shown below.

LC-MS/MS-based phospho-peptide analyses

Human NADK-FLAG immunoprecipitates were eluted with 3xFLAG peptide, separated by SDS-PAGE, stained with Coomassie Protein Stain (Expedeon), and NADK bands were excised. Coomassie stained gel pieces were reduced with 55 mM DTT, alkylated with 10 mM iodoacetamide, and digested overnight with TPCK modified trypsin (Promega) at pH 8.3. Peptides were extracted, dried in a SpeedVac, resuspended in 10 µL of 50% ACN, 6% TFA and rocked on a shaker for 15 min. Phosphopeptides were enriched by loading peptide mixture on TiO_2 tips (Poly LC) and incubated for 30 min followed by wash with 10 µl 50% ACN/1% TFA and centrifugation at 1500 rpm 0.5 min, repeated two times, eluted three times with 10 µl 40% ACN, 15% NH_4OH, added 60 µl buffer A (0.1% formic acid/99.9% water) and dried down to 5 µL. The samples were analyzed by positive ion mode LC-MS/MS using a high-resolution hybrid QExactive HF Orbitrap Mass Spectrometer (Thermo Fisher Scientific) via HCD with data-dependent analysis (DDA). Peptides were delivered and separated using an EASY-nLC nanoflow HPLC (Thermo Fisher Scientific) at 300 nL/min using self-packed 15 cm length × 75 µm i.d. C18 fritted microcapillary columns. Solvent gradient conditions were 90 minutes from 2% B buffer to 38% B (B buffer: 100% acetonitrile; A buffer: 0.9% acetonitrile/0.1% formic acid/99.0% water). MS/MS spectra were identified using Mascot Version 2.5.1 (Matrix Science) by searching the decoy and human protein database (UniProt) with a parent ion tolerance of 18 ppm and fragment ion tolerance of 0.05 Da. Carbamidomethylation of Cys (+57.0293 Da) was specified as a fixed modification and oxidation of Met (+15.9949), phosphorylation of

Ser/Thr/Tyr (+79.97) as variable modifications. Results were imported into Scaffold Q+S 4.8 software (Proteome Software) with a peptide threshold of ~80%, protein threshold of 95%, resulting in a peptide false discovery rate (FDR) of ~1%. Known contaminants such as keratins, caseins, trypsin and BSA were removed from the analysis.

Sequence Alignments

NADK amino acid sequences for different species were obtained from Uniprot (http://www.uniprot.org/). Amino acid and nucleotide sequences for human NADK isoform 1 (NADK-201, NP_075394), isoform 2 (NADK-204, NP_001185923) and isoform 3 (NADK-203, NP_001185924) were obtained from genome browser Ensembl (http://www.ensembl.org). Multiple sequence alignments were done using Clustal Omega. The alignments were visualized in Jalview (http://www.jalview.org/), where color intensity was adjusted according to the default conservation threshold value of 30.

Akt kinase assays on recombinant NADK

2 µg of bacterially-expressed GST-NADK or GST-NADK S/A variants on glutathione beads were incubated with purified His-PKB alpha (Akt1) S473D (aa 118-480) in a 50 µl reaction volume containing 50 mM Tris/HCl pH 7.5, 1 mM DTT, 0.1 mM EGTA, 10 mM magnesium acetate, 100 µM [γ-^{32}P]-ATP at 30°C for the indicated times. Akt kinase was used at 5U/ml, where one unit of protein kinase activity is the amount of enzyme that catalyzes the incorporation of 1 nmol phosphate into standard substrate in 1 min.

Mouse experiment

C57BL/6J mice were obtained from Jackson labs. 8-week-old mice were fasted for 12 hours during the light cycle (7am-7pm) and either humanely euthanized or refed in the dark cycle (7pm-7am) with a low fat/high carbohydrate diet (Harlan Teklan, TD.88122) followed by euthanization. Perigonadal fat pads were removed and frozen in liquid nitrogen. Half of this tissue was homogenized (30 seconds) with a tissue grinder in 150 µl of ice-cold 1% Triton lysis buffer supplemented with 1 µM Microcystin-LR and protease inhibitor cocktail. All animal procedures were approved by the Harvard Medical Area Institutional Animal Care and Use Committee.

Purification of bacterially-expressed NADK.

GST-NADK or S/A variants expressed from the pGEX-6P-1 vector were purified from *E. coli* BL21 after induction with 1 mM I isopropyl-β-D-thiogalactopyranoside (IPTG) for 16 hours at 28°C. Single colonies were first verified for similar expression across NADK variants and then selected clones were used for purifications. Bacterial pellets were resuspended in ice-cold resuspension buffer (50 mM HEPES pH 7.4, 140 mM NaCl, 1 mM EDTA, pH 8) supplemented with 1 mM DTT and 1:100 protease inhibitor cocktail. Lysates were produced using 0.25 mg/ml lysozyme with rocking for 15 min at 4°C, followed by another 30 min incubation at 4°C with 0.2% Triton X-100. Nucleic acids were removed by a final 30 min incubation with Benzonase. Lysates were clarified by centrifuged at 16,000g for 15 min at 4°C and supernatants were collected for subsequent purification. GST-NADK-containing lysates were incubated with glutathione beads for 2 hours at 4°C, and beads were washed three times in wash buffer (50 mM HEPES, pH 7.5, 0.2 M NaCl, 0.1% Triton X-100 supplemented with protease inhibitors) and once in PBS plus protease inhibitors. Precipitated GST-NADK was then subjected to in vitro Akt

kinase assay, or eluted from the beads after the kinase assay using 30 mM glutathione in PBS (pH 7.2) for 1 hour at 4°C for use in NADK enzymatic assays. Purified NADK was quantified on a Coomassie-stained gel with adjacent BSA standards.

NADK enzymatic assay

Approximately 0.5 µg of purified NADK or NADK variants was subjected to an NADK enzymatic assays that couples its generation of $NADP^+$ to G6PD-mediated production of NADPH, which is then measured as a change in A340 over time. The assay was performed in a 100 µl reaction in 96-well plate containing 10 mM ATP, 10 mM glucose-6-phosphate, 0.5 U G6PD, 10 mM MgCl2, 100 mM Tris-HCl (pH 8.0) and varying concentrations of the subsrate NAD^+ (1 mM, 2 mM, 5 mM, 10 mM). Measurements of A340 were made every 2 minutes for 20 min at 37^{o}C. To measure the effects of NADK phosphorylation on its enzymatic activity, NADK was subjected to *in vitro* phosphorylation by Akt as follows: HEK293E cells expressing FLAG-tagged NADK or NADK-S44/46/48A (3A) (three 15 cm dishes each) were serum-starved overnight and treated with wortmannin (200 nM) for the last hour to inhibit PI3K-Akt signaling. Cells were lysed in substrate buffer (50 mM HEPES, 250 mM NaCl, 1% Triton and 1X protease inhibitor cocktail), and NADK was immunoprecipitated for 3 hours with FLAG-affinity gel (70 µl of settled beads). After three washes in substrate buffer, NADK bound to the beads was phosphorylated with purified, active Akt in a reaction volume of 100 µl containing 50 mM Tris/HCl pH 7.5, 1 mM DTT, 0.1 mM EGTA, 10 mM magnesium acetate, 0.2 mM ATP at 30°C for 1 hour with shaking. Akt was removed by washing the beads 4 times with lysis buffer and once in equilibration buffer. NADK was then eluted with 100 µl of 3X FLAG peptide at 4^{o}C for 1 hour. 5-10% of the eluate was subjected to Coomassie staining to quantify the amount of

NADK. The reaction was then performed using ~ 0.5 µg of purified NADK. Note: cell lysates or purified NADK enzyme should not be frozen during this procedure, as freezing adversely affects NADK enzymatic activity.

Soft agar colony formation assay

For soft agar assays, 6000 cells in 2 ml of growth media (RPMI+10% FBS+2 µg/ml puromycin+ 200 µg/ml hygromycin B) containing 0.34% agarose (Lonza SeaPlaque® Agarose) were seeded in 6-well plates with a bottom layer of 0.5% agarose (prepared in the same growth media as the top layer). Cells were fed every 5 days with 0.5 ml of growth media. Colonies were detected after 4 weeks by staining with 1 ml of 0.5 mg/ml of thiazolyl Blue Tetrazolium Bromide solution for 2 hours. Colony number was determined using the OpenCFU software (http://opencfu.sourceforge.net). Images presented in the manuscript are representative of three biological replicates from two independent experiments.

Analysis of NADK isoform expression in GTEx RNA-seq data

Exon and splice junction raw count data were downloaded from The Genotype-Tissue Expression (GTEx) project (https://gtexportal.org/home/, version 7). Reads per kilobase per million reads (RPKM) values for each exon were calculated. Isoform 3 expression estimates were defined as the RPKM value for the unique first exon of Isoform-3 (chr1:1689804-1690081 (hg19 genome)). Isoform 1 expression estimates were the sum of the RPKM values mapped to two exons (chr1:1710185-1710290 and chr1:1709728-1709909) specific to the each of the splice variants that encode Isoform 1. Splice junction data was used to determine whether reads spanning the splice junctions unique to Isoform 1 (chr1:1696885:-,chr1:1710185 or

chr1:1696885:-,chr1:1709728) and Isoform 3 (chr1:1688749:-,chr1:1689804) were detected in samples.

Statistical Analysis

All error bars represent standard deviation. For pairwise comparisons, two-tailed Student's *t* tests were used. P values < 0.05 are denoted as statistically significant.

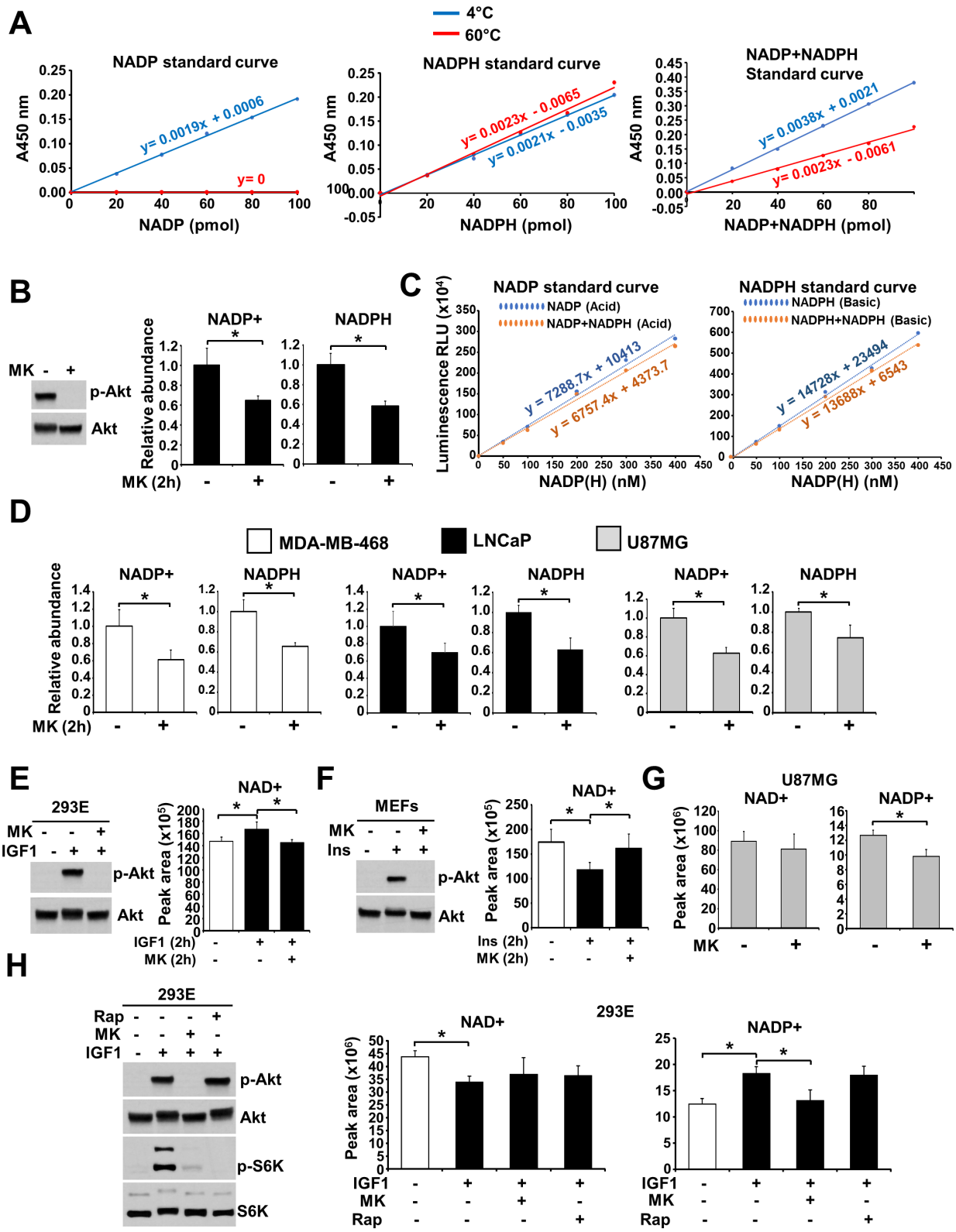
A
4°C
60°C
NADP standard curve
A450 nm
y= 0.0019x + 0.0006
y= 0
NADP (pmol)
NADPH standard curve
y= 0.0023x - 0.0065
y= 0.0021x - 0.0035
NADPH (pmol)
NADP+NADPH
Standard curve
y= 0.0038x + 0.0021
y= 0.0023x - 0.0061
NADP+NADPH (pmol)
B
MK - +
p-Akt
Akt
Relative abundance
NADP+
NADPH
MK (2h) - + - +
C
NADP standard curve
NADP (Acid)
NADP+NADPH (Acid)
Luminescence RLU (x10⁴)
y = 7288.7x + 10413
y = 6757.4x + 4373.7
NADP(H) (nM)
NADPH standard curve
NADPH (Basic)
NADP+NADPH (Basic)
y = 14728x + 23494
y = 13688x + 6543
D
MDA-MB-468
LNCaP
U87MG
Relative abundance
NADP+
NADPH
MK (2h) - + - +
E
293E
MK - - +
IGF1 - + +
p-Akt
Akt
NAD+
Peak area (x10⁵)
IGF1 (2h) - + +
MK (2h) - - +
F
MEFs
MK - - +
Ins - + +
p-Akt
Akt
NAD+
Peak area (x10⁵)
Ins (2h) - + +
MK (2h) - - +
G
U87MG
NAD+
NADP+
Peak area (x10⁶)
MK - +
H
293E
Rap - - - +
MK - - + -
IGF1 - + + +
p-Akt
Akt
p-S6K
S6K
NAD+
Peak area (x10⁶)
293E
NADP+
IGF1 - + + +
MK - - + -
Rap - - - +

Fig. S1. Data supporting Figure 1A-E.

(**A**) Standard curves were generated from pure $NADP^+$ and NADPH standards that, where indicated, were subjected to heating (60°C, 30 min) to decompose NADP. Increasing concentrations of $NADP^+$ (left), NADPH (middle), and a 1:1 mixture of NADP and NADPH (right) were measured using the NADP/NADPH quantification assay used in Fig. 1A-C (see methods).

(**B**) Relative abundance of $NADP^+$ and NADPH from HEK293E cells grow in full serum (10% FBS) and treated for 2 hours with vehicle (DMSO) or MK-2206 (2 μM) were quantified as in (A). Data are presented as the mean ± SD of biological quintuplicates.

(**C**) Standard curves were generated from pure $NADP^+$ and NADPH and a 1:1 mixture of NADP and NADPH using a bioluminescent enzyme-based assay. Samples were subjected to acidic and basic extraction for specifically measuring NADP and NADPH, respectively (see methods).

(**D**) Relative abundance of $NADP^+$ and NADPH from PTEN-deficient cell lines, serum-deprived 16 hours and treated 2 hours with vehicle or MK-2206 (2 μM) were quantified as in (C). Data are presented as the mean ± SD of biological quintuplicates.

(**E, F**). Immunoblots and normalized peak areas of NAD^+ from the experimental samples in Fig. 1D (E) and 1E (F).

(**G**) Normalized peak areas of NAD^+ and $NADP^+$ measured by targeted LC-MS/MS from U87MG cells serum-deprived for 16 hours and treated with 2 μM MK-2206 for the last 2 hours.

(**H**) Immunoblots and normalized peak areas of NAD^+ and $NADP^+$ measured by targeted LC-MS/MS from HEK293E cells that were serum-starved for 16 hours and pretreated with MK-2206 (2 μM, 30 min) or rapamycin (20 nM, 30 min) prior to stimulation with IGF1 (100ng/ml, 1 hour).

(**B, G, H**) Data are presented as the mean ± SD of biological quadruplicates and are representative of two independent experiments. *P < 0.05 for pairwise comparisons calculated using a two-tailed Student's t-test.

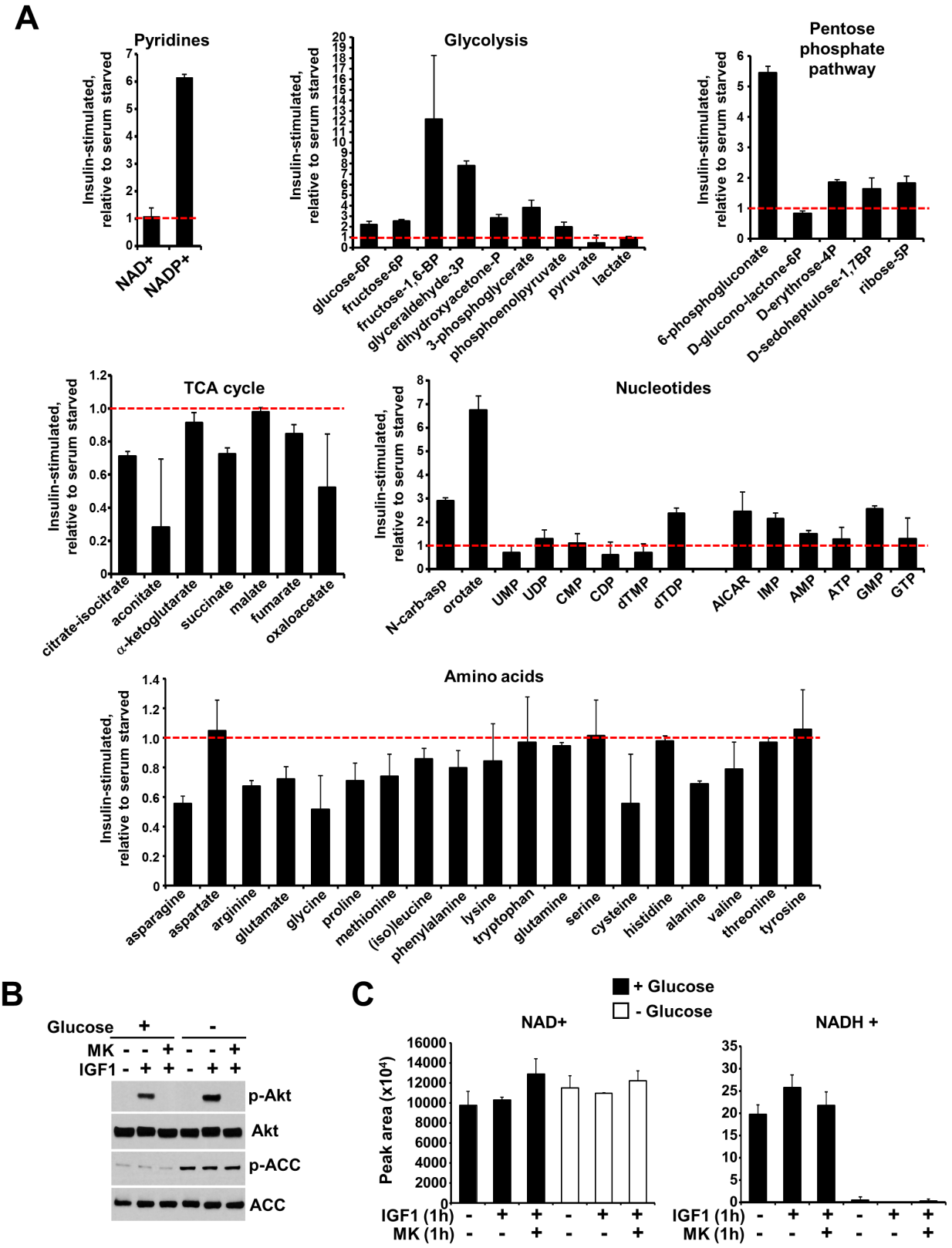
A
Pyridines
Insulin-stimulated, relative to serum starved
NAD+
NADP+
Glycolysis
glucose-6P
fructose-6P
fructose-1,6-BP
glyceraldehyde-3P
dihydroxyacetone-P
3-phosphoglycerate
phosphoenolpyruvate
pyruvate
lactate
Pentose phosphate pathway
6-phosphogluconate
D-glucono-lactone-6P
D-erythrose-4P
D-sedoheptulose-1,7BP
ribose-5P
TCA cycle
citrate-isocitrate
aconitate
α-ketoglutarate
succinate
malate
fumarate
oxaloacetate
Nucleotides
N-carb-asp
orotate
UMP
UDP
CMP
CDP
dTMP
dTDP
AICAR
IMP
AMP
ATP
GMP
GTP
Amino acids
asparagine
aspartate
arginine
glutamate
glycine
proline
methionine
(iso)leucine
phenylalanine
lysine
tryptophan
glutamine
serine
cysteine
histidine
alanine
valine
threonine
tyrosine
B
Glucose + -
MK - - + - - +
IGF1 - + + - + +
p-Akt
Akt
p-ACC
ACC
C
+ Glucose
- Glucose
NAD+
NADH +
Peak area (x10⁴)
IGF1 (1h) - + + - + +
MK (1h) - - + - - +

Fig. S2. Data supporting Figure 1

(**A**) HeLa cells were deprived of serum (15 hours) and then treated with insulin (0.5 μM, 1 hour). The indicated metabolites measured by targeted LC-MS/MS are shown as insulin-stimulated abundance relative to unstimulated, indicated by the dashed red line.

(**B, C**) Immunoblots (B) and normalized peak areas of NAD^+ and NADH from the experimental samples in Fig. 1F (C).

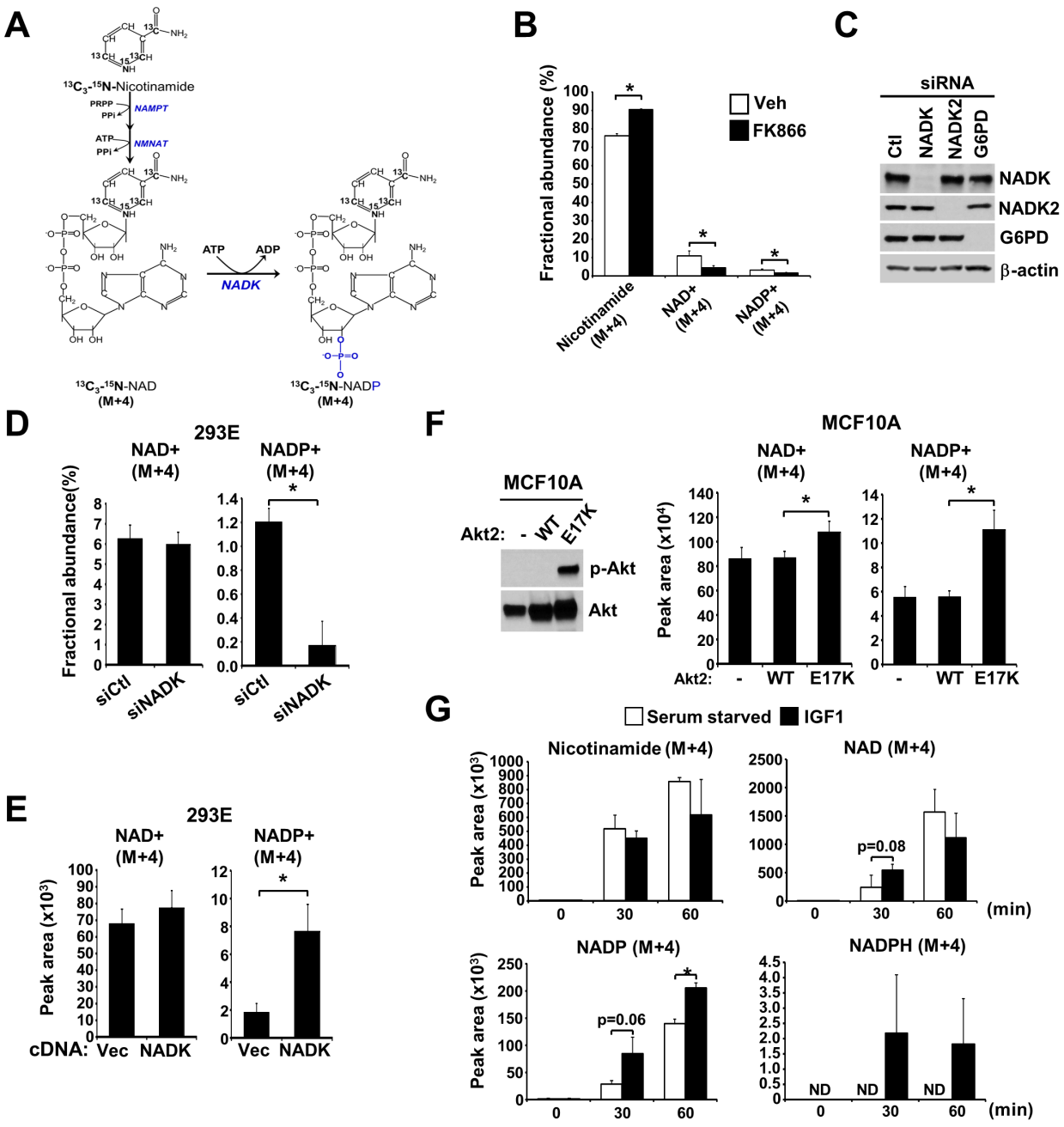
A
$^{13}C_3$-^{15}N-Nicotinamide
PRPP
PPi
NAMPT
ATP
PPi
NMNAT
ATP
ADP
NADK
$^{13}C_3$-^{15}N-NAD (M+4)
$^{13}C_3$-^{15}N-NADP (M+4)
B
Fractional abundance (%)
Veh
FK866
Nicotinamide (M+4)
NAD+ (M+4)
NADP+ (M+4)
C
siRNA
Ctl
NADK
NADK2
G6PD
NADK
NADK2
G6PD
β-actin
D
293E
NAD+ (M+4)
NADP+ (M+4)
Fractional abundance(%)
siCtl
siNADK
siCtl
siNADK
E
293E
NAD+ (M+4)
NADP+ (M+4)
Peak area (x10^3)
cDNA: Vec NADK
Vec NADK
F
MCF10A
MCF10A
Akt2: - WT E17K
p-Akt
Akt
MCF10A
NAD+ (M+4)
NADP+ (M+4)
Peak area (x10^4)
Akt2: - WT E17K
- WT E17K
G
Serum starved
IGF1
Nicotinamide (M+4)
NAD (M+4)
Peak area (x10^3)
p=0.08
(min)
NADP (M+4)
NADPH (M+4)
Peak area (x10^3)
p=0.06
ND
ND
ND
(min)

Fig. S3. Data supporting Figure 1G-K.

(**A**) Schematic of the NAD salvage pathway and $^{13}C_3$-^{15}N-nicotinamide stable-isotope tracing into NAD^+ and $NADP^+$, which results in the appearance of M+4 mass isotopomers of these metabolites. PRPP: phosphoribosyl pyrophosphate.

(**B**) Fractional abundance (%) of nicotinamide (M+4), NAD^+ (M+4) and $NADP^+$ (M+4) from the experimental samples in Fig. 1H are shown.

(**C**) Immunoblots were performed in parallel samples prepared as described in Fig. 1I.

(**D**) Fractional abundance (%) of NAD^+ (M+4) and $NADP^+$ (M+4) from Fig. 1I.

(**E**) HEK293E cells transfected with empty vector (Vec) or NADK for 24 hours were grown in full serum and labeled with $^{13}C_3$-^{15}N-nicotinamide for 1 hour. Normalized peak areas of NAD^+ (M+4) and $NADP^+$ (M+4) were measured by targeted LC-MS/MS.

(**F**) MCF10A cells stably expressing empty vector (-), Akt2 (WT) or oncogenic Akt2 (E17K) in a doxycycline-inducible manner were cultured in the presence of doxycycline (0.15 μg/ml, 36 hours). Cells were serum deprived for 16 hours in the presence of doxycycline (0.15 μg/ml) and labeled with $^{13}C_3$-^{15}N-nicotinamide media for the final 1 hour. Normalized peak areas of NAD^+ (M+4) and $NADP^+$ (M+4) were measured by targeted LC-MS/MS.

(**G**) HEK293E cells were serum deprived for 16 hours prior to IGF1 (100 ng/ml) and $^{13}C_3$-^{15}N-nicotinamide labelling for the indicated times. Normalized peak areas of nicotinamide (M+4), NAD^+ (M+4), $NADP^+$ (M+4) and NADPH (M+4) were measured by targeted LC-MS/MS.

(**E-G**) Data are presented as the mean ± SD of biological quadruplicates and are representative of two independent experiments. *$P < 0.05$ for pairwise comparisons calculated using a two-tailed Student's t-test.

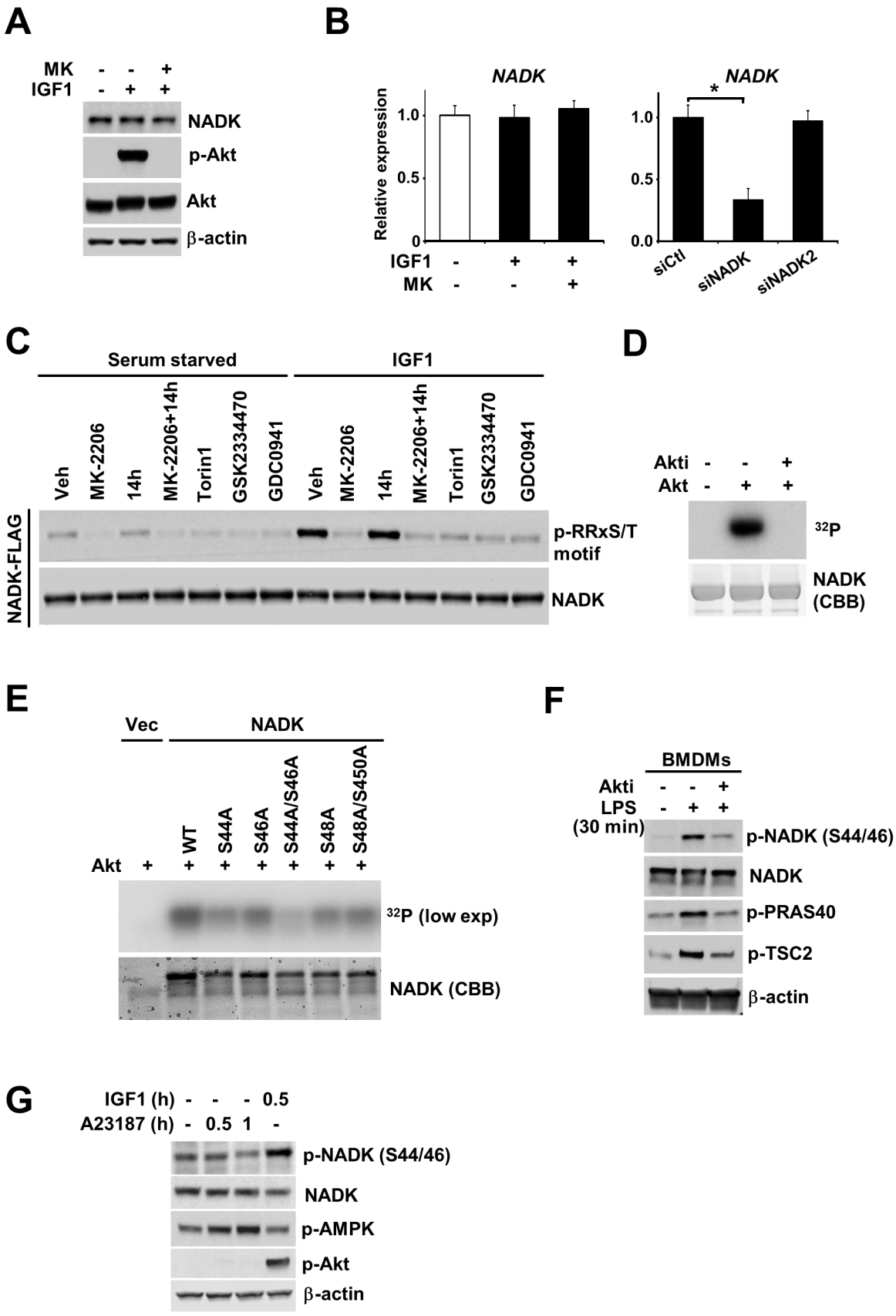
A
MK - - +
IGF1 - + +
NADK
p-Akt
Akt
β-actin
B
NADK
Relative expression
1.0
0.5
0
IGF1 - + +
MK - - +
NADK
*
1.0
0.5
0.0
siCtl
siNADK
siNADK2
C
Serum starved
IGF1
Veh
MK-2206
14h
MK-2206+14h
Torin1
GSK2334470
GDC0941
NADK-FLAG
p-RRxS/T motif
NADK
D
Akti - - +
Akt - + +
32P
NADK (CBB)
E
Vec
NADK
WT
S44A
S46A
S44A/S46A
S48A
S48A/S450A
Akt +
32P (low exp)
NADK (CBB)
F
BMDMs
Akti - - +
LPS - + +
(30 min)
p-NADK (S44/46)
NADK
p-PRAS40
p-TSC2
β-actin
G
IGF1 (h) - - - 0.5
A23187 (h) - 0.5 1 -
p-NADK (S44/46)
NADK
p-AMPK
p-Akt
β-actin

Fig. S4. Data supporting Figure 2.

(**A**) Immunoblot from HEK293E cells serum-deprived overnight and pretreated with MK-2206 (2 μM, 30 min) prior to treatment with IGF1 (100 ng/ml, 2 hour).

(**B**) The relative abundance of NADK transcripts are shown for samples treated as in (A) or following siRNA-mediated knockdown of NADK or NADK2. Data are graphed as mean ± SD of biological triplicates and are representative of two independent experiments. *P < 0.05 by two-tailed Student's t test.

(**C**) FLAG-tagged NADK was immunoprecipitated from HEK293E cells deprived of serum for 16 hours, pretreated for 30 min with vehicle (Veh), Akt inhibitor MK-2206 (2 μM), SGK1 inhibitor 14h (1 μM), mTOR catalytic inhibitor Torin1 (250 nM), PDK1 inhibitor GSK2334470 (1 μM), or pan-PI3K inhibitor GDC-0941 (1 μM) prior to treatment with IGF1 (100 ng/ml, 30 min). NADK phosphorylation was detected using the indicated phospho-motif antibody.

(**D**) In vitro kinase assays were performed using recombinant active Akt1 and bacterially-purified GST-NADK in the presence of [γ-^{32}P] ATP and the ATP-competitive Akt inhibitor GSK690693 (5 μM), where indicated. Reactions were stopped after 15 minutes and detected by autoradiography. CBB, Coomassie brilliant blue showing total NADK in the reaction.

(**E**) As in (D), but NADK-FLAG or the indicated S/A mutants were immunopurified from serum-deprived HEK293E cells treated with the PI3K inhibitor wortmannin (200 nM, 1 hour).

(**F**) Endogenous NADK was detected with a phospho-NADK (S44/46) antibody in lysates of primary BMDMs that were pretreated with the Akt inhibitor GSK690693 (5 μM, 30 min) prior to stimulation with LPS (100 ng/ml, 30 min).

(**G**) Endogenous NADK phosphorylation was detected in HEK293E cells serum deprived for 16 hours prior to treatment with the calcium ionophore A23187 (10 μM) and IGF1 (100 ng/ml) for

the indicated times. Phospho-AMPK (T172) is a positive control for $Ca2^{+}$-dependent phosphorylation upon A23187 treatment.

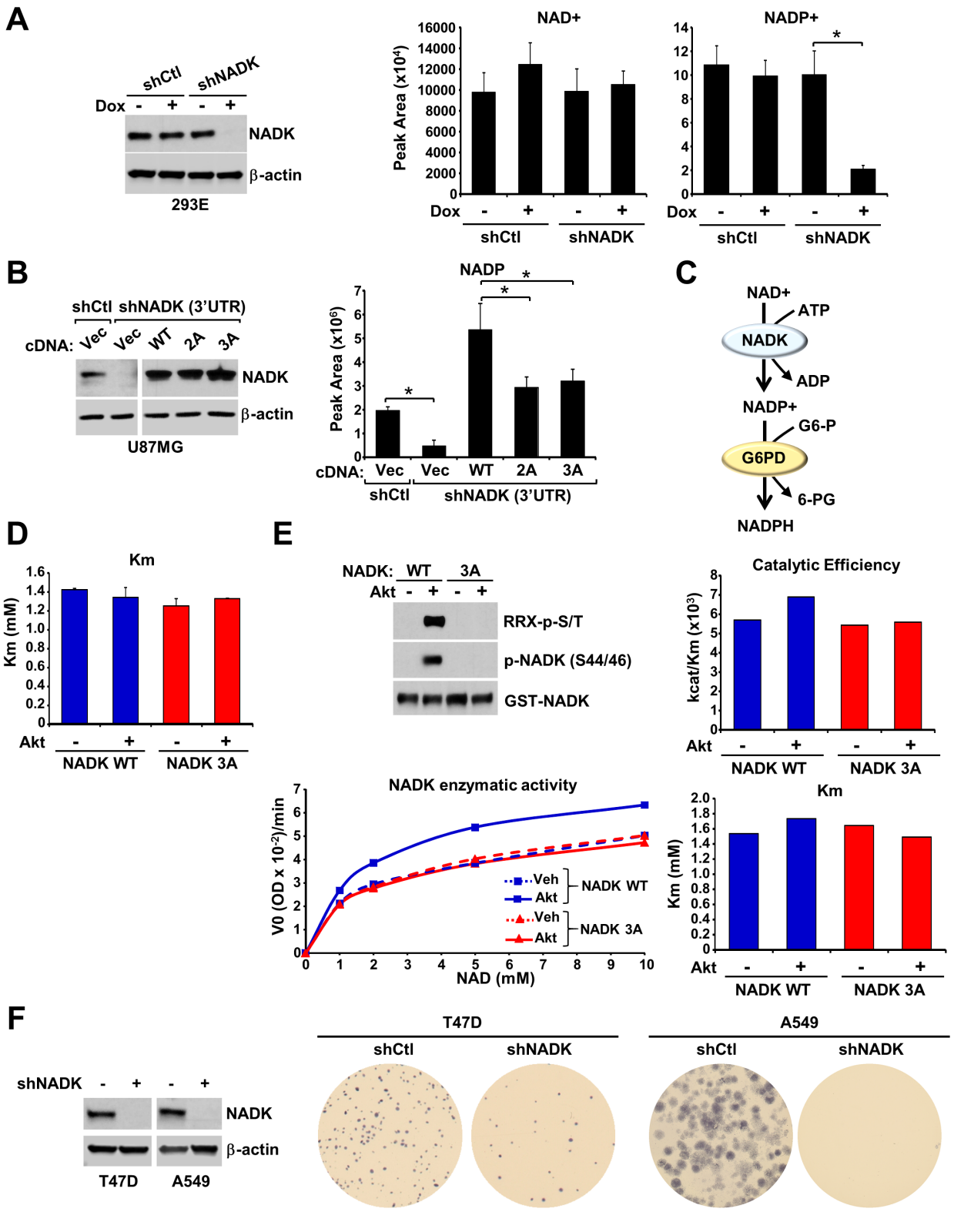
A
shCtl
shNADK
Dox - + - +
NADK
β-actin
293E
NAD+
Peak Area (x10⁴)
16000
14000
12000
10000
8000
6000
4000
2000
0
Dox - + - +
shCtl
shNADK
NADP+
*
14
12
10
8
6
4
2
0
Dox - + - +
shCtl
shNADK
B
shCtl shNADK (3'UTR)
cDNA: Vec Vec WT 2A 3A
NADK
β-actin
U87MG
NADP
*
*
Peak Area (x10⁶)
7
6
5
4
3
2
1
0
cDNA: Vec Vec WT 2A 3A
shCtl
shNADK (3'UTR)
C
NAD+
ATP
NADK
ADP
NADP+
G6-P
G6PD
6-PG
NADPH
D
Km
Km (mM)
1.6
1.4
1.2
1.0
0.8
0.6
0.4
0.2
0
Akt - + - +
NADK WT
NADK 3A
E
NADK: WT 3A
Akt - + - +
RRX-p-S/T
p-NADK (S44/46)
GST-NADK
Catalytic Efficiency
kcat/Km (x10³)
8
7
6
5
4
3
2
1
0
Akt - + - +
NADK WT
NADK 3A
NADK enzymatic activity
V0 (OD x 10⁻²)/min
7
6
5
4
3
2
1
0
0 1 2 3 4 5 6 7 8 9 10
NAD (mM)
Veh
Akt
NADK WT
Veh
Akt
NADK 3A
Km
Km (mM)
2.0
1.8
1.6
1.4
1.2
1.0
0.8
0.6
0.4
0.2
0
Akt - + - +
NADK WT
NADK 3A
F
shNADK - + - +
NADK
β-actin
T47D
A549
T47D
shCtl
shNADK
A549
shCtl
shNADK

Fig. S5. Data supporting Figure 3.

(**A**) HEK293E cells stably expressing doxycycline-inducible control shRNA (shCtl) or shRNA targeting the 3'UTR of NADK were cultured in the presence or absence of doxycycline (0.25 μg/ml, 48 hours). Immunoblots and normalized peak areas of NAD^+ and $NADP^+$ measured by targeted LC-MS/MS are shown.

(**B**) U87MG cells with stable shRNA-mediated knockdown of NADK were stably transfected with empty vector (Vec), NADK (WT), or NADK phospho-mutants S44/46A (2A) or S44/46/48A (3A). Cells were grown in the presence of doxycycline (0.25 μg/ml, 36 hours) and serum deprived (16 hours) in the presence of doxycycline. Immunoblots and normalized peak areas of $NADP^+$ are shown. (A, B) Data are presented as the mean ± SD of biological quadruplicates and are representative of two independent experiments. *$P < 0.05$ for pairwise comparisons calculated using a two-tailed Student's t-test.

(**C**) Schematic of the coupled NADK enzymatic assay employed in which NADK-produced $NADP^+$ is used by purified G6PD to generate NADPH, which is measured by spectrophotometric absorbance at A340.

(**D**) K_m of NADK-WT and -3A for NAD^+ calculated from the experiment shown Fig. 3D-F.

(**E**) Recombinant, bacterially purified NADK-WT or 3A mutant was phosphorylated with purified active Akt in vitro and subjected to immunoblot and an assay of NADK activity measured over a range of NAD^+ concentrations (see methods for more details).

(**F**) Soft agar colony formation assay from T47D and A549 cells with stable shRNA-mediated knockdown of NADK. Images from T47D cells were magnified by 3X. Images presented are representative of two independent experiments performed in biological triplicates. Immunoblots show NADK levels.

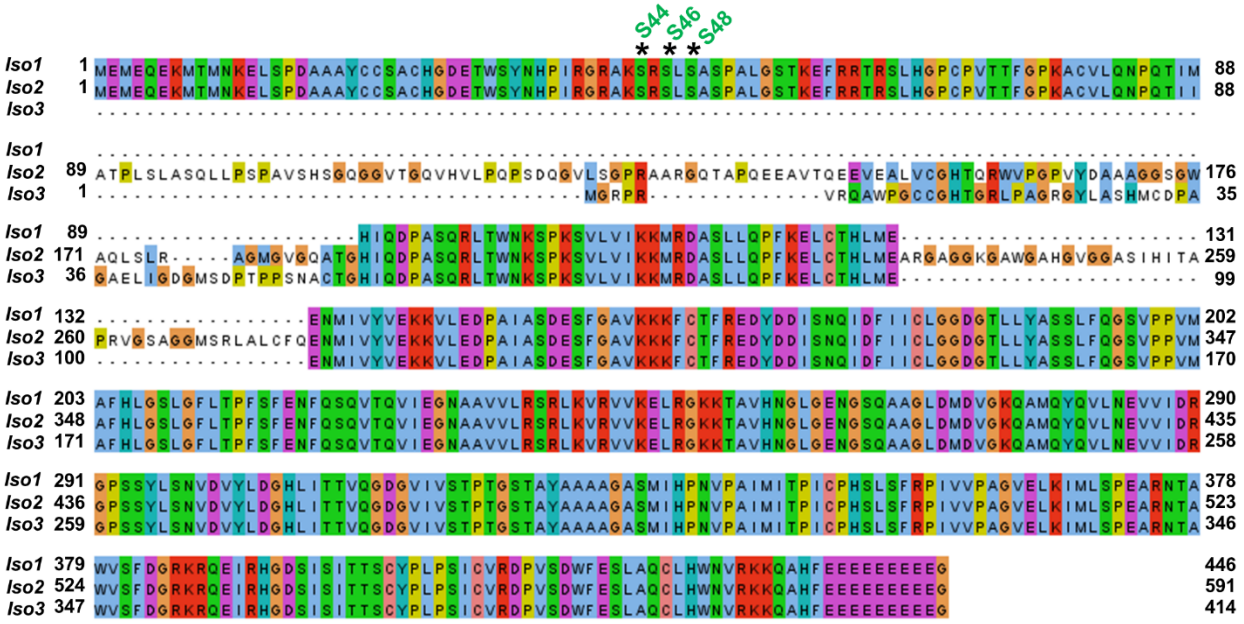

Fig. S6. NADK sequence alignment supporting Figure 4.

Sequence alignment of human NADK isoform 1 (NP_075394; Iso1), isoform 2 (NP_001185923; Iso2), and isoform 3 (NP_001185924; Iso3) using Clustal Omega, with the Akt phosphorylation sites (S44, S46, S48) denoted within the N-terminal regulatory domain shared between isoforms 1 and 2, but absent from predicted isoform 3.

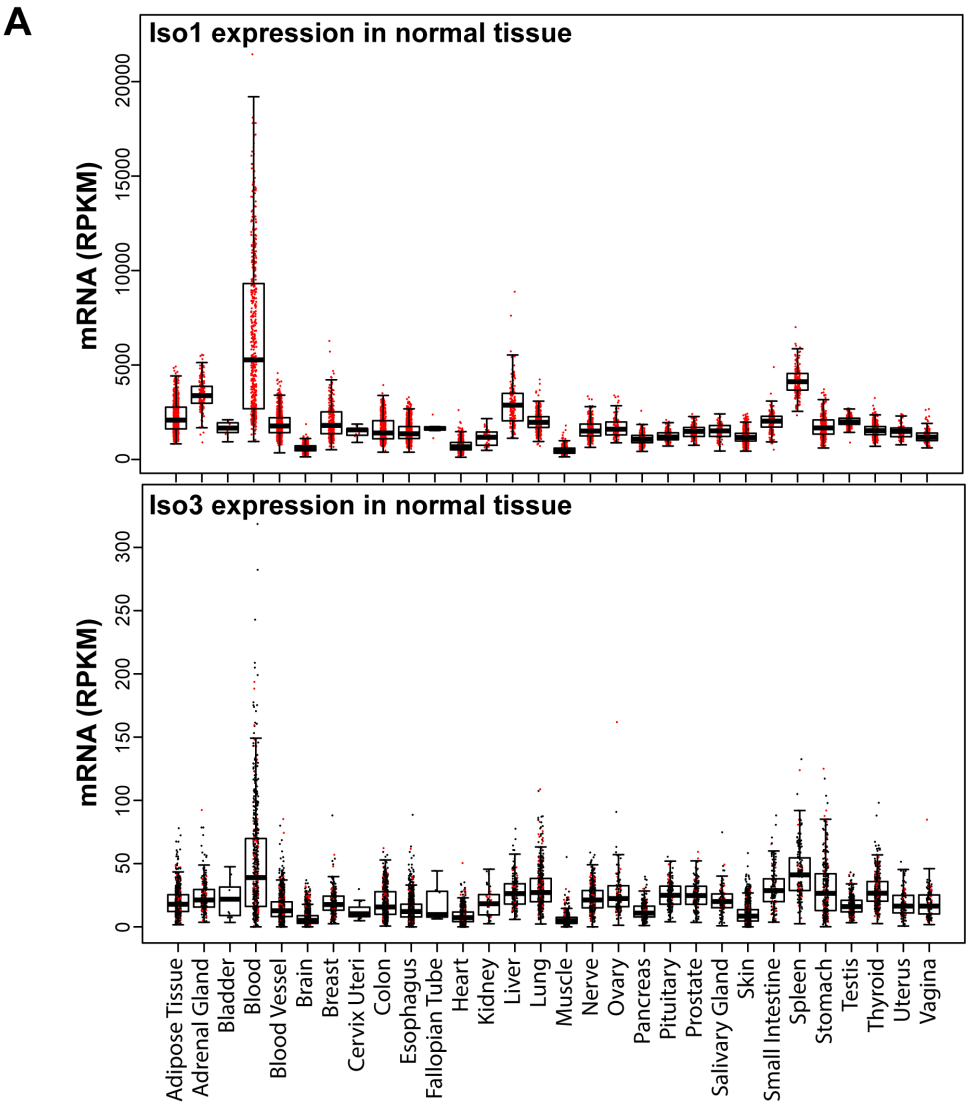
A
Iso1 expression in normal tissue
mRNA (RPKM)
0
5000
10000
15000
20000
Iso3 expression in normal tissue
mRNA (RPKM)
0
50
100
150
200
250
300
Adipose Tissue
Adrenal Gland
Bladder
Blood
Blood Vessel
Brain
Breast
Cervix Uteri
Colon
Esophagus
Fallopian Tube
Heart
Kidney
Liver
Lung
Muscle
Nerve
Ovary
Pancreas
Pituitary
Prostate
Salivary Gland
Skin
Small Intestine
Spleen
Stomach
Testis
Thyroid
Uterus
Vagina

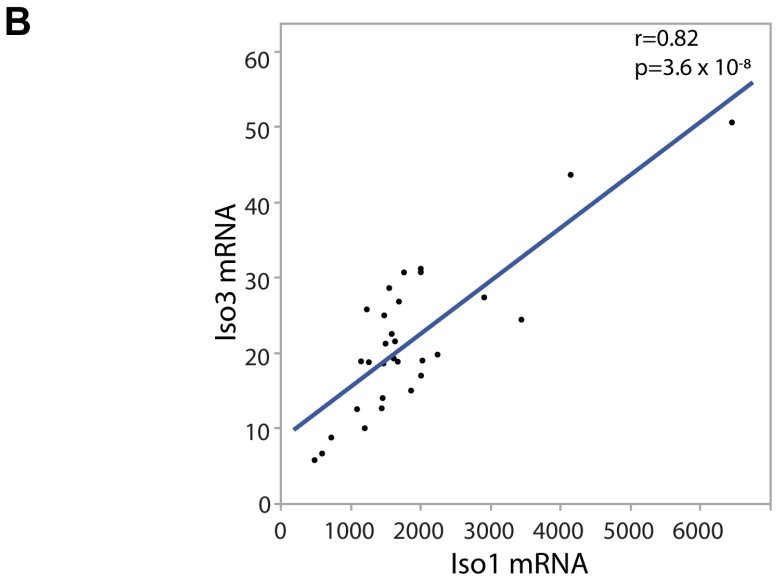
B
r=0.82
p=3.6 x 10-8
Iso3 mRNA
0
10
20
30
40
50
60
0
1000
2000
3000
4000
5000
6000
Iso1 mRNA

Fig. S7. RNA-seq data from GTEx for NADK isoforms 1 and 3, demonstrating the existence but low expression of isoform 3 transcripts.

(**A**) mRNA abundance, expressed as reads per kilobase per million reads (RPKM), for NADK isoform 1 (top) and isoform 3 (bottom) from a range of normal tissues. Each dot represents a tissue sample; red dots indicate the detection of a read that spans an isoform-specific splice junction. Boxes define the interquartile range (IQR), the horizontal line indicates the median, and the whiskers represent the upper and lower quartiles +/- 1.5 x IQR.

(**B**) Correlation between NADK isoform 1 (Iso1) and isoform 3 (Iso3) expression showing high correlation across tissues (r=0.82, p=3.6 x 10-8, Pearson's correlation).

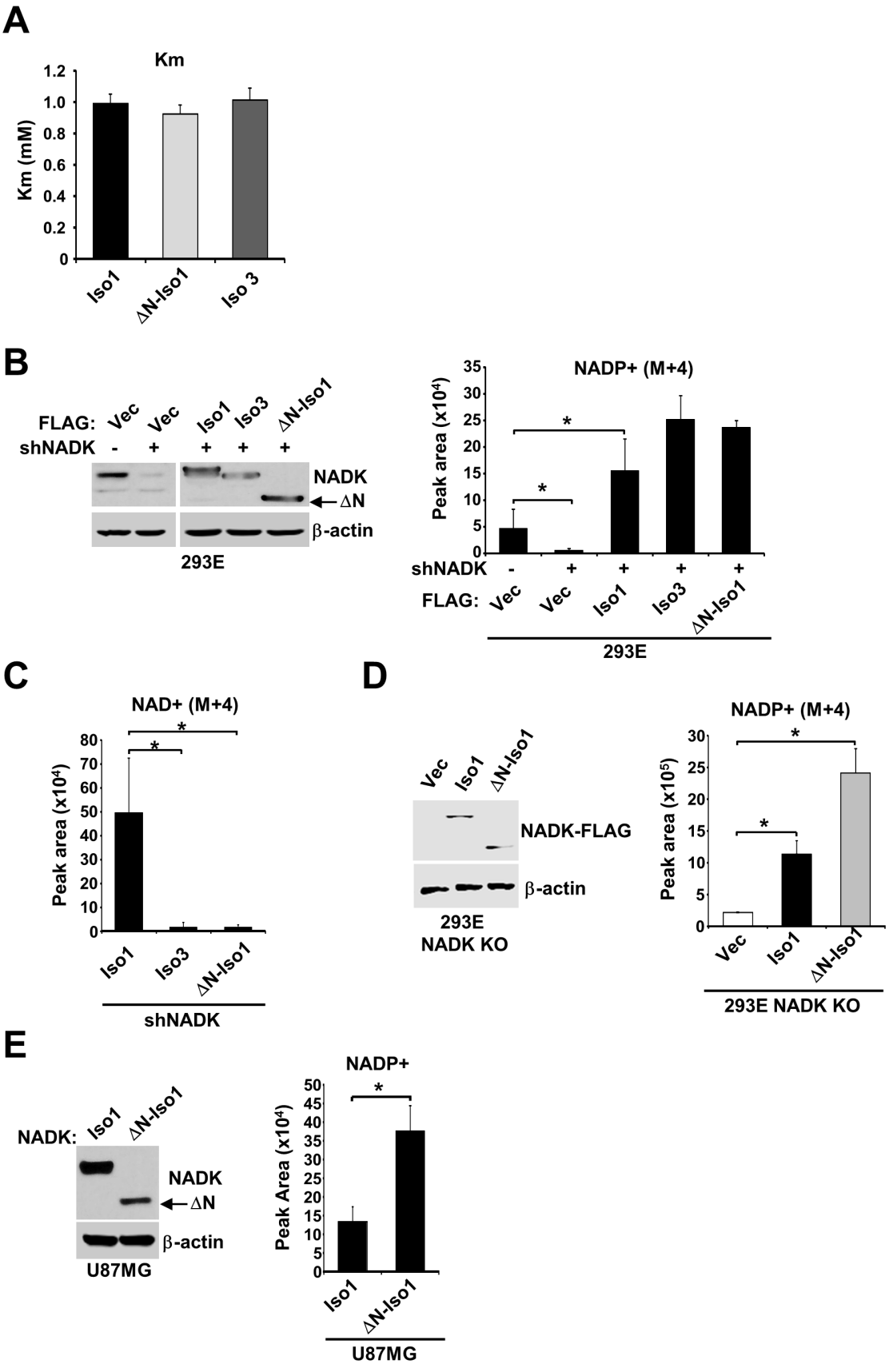
A
Km
Km (mM)
1.2
1.0
0.8
0.6
0.4
0.2
0
Iso1
ΔN-Iso1
Iso 3
B
FLAG: Vec Vec Iso1 Iso3 ΔN-Iso1
shNADK - + + + +
NADK
←ΔN
β-actin
293E
NADP+ (M+4)
Peak area (x10⁴)
35
30
25
20
15
10
5
0
*
*
shNADK - + + + +
FLAG: Vec Vec Iso1 Iso3 ΔN-Iso1
293E
C
NAD+ (M+4)
Peak area (x10⁴)
80
70
60
50
40
30
20
10
0
*
*
Iso1
Iso3
ΔN-Iso1
shNADK
D
Vec
Iso1
ΔN-Iso1
NADK-FLAG
β-actin
293E
NADK KO
NADP+ (M+4)
Peak area (x10⁵)
30
25
20
15
10
5
0
*
*
Vec
Iso1
ΔN-Iso1
293E NADK KO
E
NADK: Iso1 ΔN-Iso1
NADK
←ΔN
β-actin
U87MG
NADP+
Peak Area (x10⁴)
50
45
40
35
30
25
20
15
10
5
0
*
Iso1
ΔN-Iso1
U87MG

Fig. S8. Data supporting Figure 4B and C.

(**A)** K_m of NADK isoforms for NAD^+ calculated from the experiment shown in Fig. 4B.

(**B, C**) NADK-isoform 1, -isoform 3 or -ΔN-isoform 1 (lacking aa 1-87) were transfected into HEK293E cells with stable shRNA knockdown of endogenous NADK for 24 hours prior to serum-deprivation (16 hours) and labelling for the last hour with $^{13}C_3$-^{15}N-nicotinamide. Normalized mean peak areas of labeled (M+4) $NADP^+$ (B) and (M+4) NAD^+ (C) are graphed.

(**D**) Empty vector (Vec), NADK-isoform 1 or ΔN-NADK-isoform1 were stably expressed in NADK-null HEK293 cells generated via CRISPR/Cas9 gene editing. Cells were serum-deprived overnight and labeled for 1 hour with $^{13}C_3$-^{15}N-nicotinamide to measure basal $NADP^+$ synthesis. Normalized mean peak areas of labeled (M+4) $NADP^+$ are graphed.

(**E**) Normalized peak areas of $NADP^+$ measured by targeted LC-MS/MS from U87MG cells stably expressing shRNAs targeting the 3'UTR of NADK and exogenous cDNAs of NADK-isoform 1 or the ΔN-isoform 1 mutant, grown under serum-deprived conditions for 16 hours.

(**B-E**) Data are presented as the mean ± SD of biological quadruplicates and are representative of two independent experiments. *$P < 0.05$ for pairwise comparisons calculated using a two-tailed Student's t-test.

Table S1. Selective Ion Monitoring (SIM) of metabolites measured for stable isotopic tracing ($^{13}C_3$-^{15}N-nicotinamide).

CompoundName	Chemical Formula	Ionization	Polarity	ChargeState
Nicotinamide +	C6H6N2O	ESI	+	1
Nicotinamide_13C3_15N +	[13]C3C3H6[15]N1NO	ESI	+	1
NAD +	C21H28N7O14P2	ESI	+	1
NAD+_13C3_15N +	[13]C3C18H28[15]NN6O14P2	ESI	+	1
NADP +	C21H29N7O17P3	ESI	+	1
NADP+_13C3_15N +	[13]C3C18H29[15]NN6O17P3	ESI	+	1
NADPH +	C21H30N7O17P3	ESI	+	1
NADPH_13C3_15N+	[13]C3C18H30[15]NN6O17P4	ESI	+	1

Table S2: Primers used to detect human NADK and NADK2

Primer	Forward Sequence	Reverse Sequence
NADK	CGACGGAGTGATCGTGTCC	GTGTTCCTTGCTTCAGGTGAC
NADK2	ACAGAAGTTCTATCGTGGTGAGT	AGCTCTTTCAATGTTAAGGGCTC
RPLP0	CAGATTGGCTACCCAACTGTT	GGGAAGGTGTAATCCGTCTCC

References and Notes

1. I. Ben-Sahra, B. D. Manning, mTORC1 signaling and the metabolic control of cell growth. *Curr. Opin. Cell Biol.* **45**, 72–82 (2017). doi:10.1016/j.ceb.2017.02.012 Medline

2. B. D. Manning, A. Toker, AKT/PKB signaling: Navigating the network. *Cell* **169**, 381–405 (2017). doi:10.1016/j.cell.2017.04.001 Medline

3. L. Agledal, M. Niere, M. Ziegler, The phosphate makes a difference: Cellular functions of NADP. *Redox Rep.* **15**, 2–10 (2010). doi:10.1179/174329210X12650506623122 Medline

4. R. C. Stanton, Glucose-6-phosphate dehydrogenase, NADPH, and cell survival. *IUBMB Life* **64**, 362–369 (2012). doi:10.1002/iub.1017 Medline

5. R. J. DeBerardinis, N. S. Chandel, Fundamentals of cancer metabolism. *Sci. Adv.* **2**, e1600200 (2016). doi:10.1126/sciadv.1600200 Medline

6. H. Hirai, H. Sootome, Y. Nakatsuru, K. Miyama, S. Taguchi, K. Tsujioka, Y. Ueno, H. Hatch, P. K. Majumder, B.-S. Pan, H. Kotani, MK-2206, an allosteric Akt inhibitor, enhances antitumor efficacy by standard chemotherapeutic agents or molecular targeted drugs in vitro and in vivo. *Mol. Cancer Ther.* **9**, 1956–1967 (2010). doi:10.1158/1535-7163.MCT-09-1012 Medline

7. I. Ben-Sahra, J. J. Howell, J. M. Asara, B. D. Manning, Stimulation of de novo pyrimidine synthesis by growth signaling through mTOR and S6K1. *Science* **339**, 1323–1328 (2013). doi:10.1126/science.1228792 Medline

8. A. M. Robitaille, S. Christen, M. Shimobayashi, M. Cornu, L. L. Fava, S. Moes, C. Prescianotto-Baschong, U. Sauer, P. Jenoe, M. N. Hall, Quantitative phosphoproteomics reveal mTORC1 activates de novo pyrimidine synthesis. *Science* **339**, 1320–1323 (2013). doi:10.1126/science.1228771 Medline

9. L. Liu, X. Su, W. J. Quinn 3rd, S. Hui, K. Krukenberg, D. W. Frederick, P. Redpath, L. Zhan, K. Chellappa, E. White, M. Migaud, T. J. Mitchison, J. A. Baur, J. D. Rabinowitz, Quantitative analysis of NAD synthesis-breakdown fluxes. *Cell Metab.* **27**, 1067–1080.e5 (2018). doi:10.1016/j.cmet.2018.03.018 Medline

10. N. Pollak, M. Niere, M. Ziegler, NAD kinase levels control the NADPH concentration in human cells. *J. Biol. Chem.* **282**, 33562–33571 (2007). doi:10.1074/jbc.M704442200 Medline

11. N. R. Love, N. Pollak, C. Dölle, M. Niere, Y. Chen, P. Oliveri, E. Amaya, S. Patel, M. Ziegler, NAD kinase controls animal NADP biosynthesis and is modulated via evolutionarily divergent calmodulin-dependent mechanisms. *Proc. Natl. Acad. Sci. U.S.A.* **112**, 1386–1391 (2015). doi:10.1073/pnas.1417290112 Medline

12. E. C. Lien, C. A. Lyssiotis, A. Juvekar, H. Hu, J. M. Asara, L. C. Cantley, A. Toker, Glutathione biosynthesis is a metabolic vulnerability in PI(3)K/Akt-driven breast cancer. *Nat. Cell Biol.* **18**, 572–578 (2016). doi:10.1038/ncb3341 Medline

13. V. Byles, A. J. Covarrubias, I. Ben-Sahra, D. W. Lamming, D. M. Sabatini, B. D. Manning, T. Horng, The TSC-mTOR pathway regulates macrophage polarization. *Nat. Commun.* **4**, 2834 (2013). doi:10.1038/ncomms3834 Medline

14. I. Ben-Sahra, G. Hoxhaj, S. J. H. Ricoult, J. M. Asara, B. D. Manning, mTORC1 induces purine synthesis through control of the mitochondrial tetrahydrofolate cycle. *Science* **351**, 728–733 (2016). doi:10.1126/science.aad0489 Medline

15. C. A. Lewis, S. J. Parker, B. P. Fiske, D. McCloskey, D. Y. Gui, C. R. Green, N. I. Vokes, A. M. Feist, M. G. Vander Heiden, C. M. Metallo, Tracing compartmentalized NADPH metabolism in the cytosol and mitochondria of mammalian cells. *Mol. Cell* **55**, 253–263 (2014). doi:10.1016/j.molcel.2014.05.008 Medline

16. M. Yuan, S. B. Breitkopf, X. Yang, J. M. Asara, A positive/negative ion-switching, targeted mass spectrometry-based metabolomics platform for bodily fluids, cells, and fresh and fixed tissue. *Nat. Protoc.* **7**, 872–881 (2012). doi:10.1038/nprot.2012.024 Medline